

# STUDY OF LOW ENERGY NUCLEAR REACTIONS IN EXPERIMENTS WITH HYDROGEN / DEUTERIUM LOADED METALIC CATHODES IN ELECTRIC DISCHARGES

A.B.Karabut

FSUE “LUCH”, 24 Zheleznodorozhnaya St, Podolsk, Moscow Region, 142100,  
Russia.

Tel. (095) 5508129; Fax (095) 5508129; E-mail [7850.g23@g23.relcom.ru](mailto:7850.g23@g23.relcom.ru)

Experimental research of heat, high-energy and nuclear processes occurring in the cathode solid medium in electric discharge systems is presented. The obtained values of Excess Heat power in experiments with Glow Discharge and High-Voltage Electrolysis amount to 5 – 15 W and 180-280 W (up to 1000 V), respectively. The estimated Efficiency proved to be about 160% for GD experiments, and up to 800% for HVE experiments, respectively. Production of the impurity nuclides (nuclear ash) with atomic masses less than and more than that of the cathode material was registered.

X-ray emission was recorded during the GD operation and after the GD current switch off. Presumably the observed X-ray emission results from deactivation of long-lived excited energetic states in the cathode solid medium. The said excited energetic states (ranging 0.5 – 10.0 keV) formed in the cathode solid medium trigger LENR which leads to production of Excess Heat power and nuclear ash. Analysis of these results allows one to assess possible basic processes going on in the cathode material exposed to the electric discharge systems.

A theoretical assumption of the phenomena leading to generation of EH power and nuclear transmutation products in the cathode solid medium is considered.

## 1.EXCESS HEAT REGISTRATION

### 1.1. Excess Heat Registration in Glow Discharge Experiments

Measurements of EH power were carried out in experiments with pulse-periodic high-current GD device. The highest EH power values ranging 5 – 15 W with Efficiency up to 160% were recorded when the GD operational voltage ranged 1000 - 1300 V (Fig.1a,b).

Thus, it was experimentally established, that the EH power production was predetermined by two conditions: 1) deuterium should be loaded into the solid-state crystal lattice medium; 2) the crystal lattice should get initial excitation, so that high-energy long-lived excited levels should be created in the cathode sample solid. These excited conditions could be induced by an additional source (for example by a flux of inert gas ions).

### 1.1. Excess Heat Registration in High-Voltage Electrolysis Experiments

The Glow Discharge results are in good agreement with Excess Heat measurements obtained in experiments with high-voltage electrolysis at cathode-anode voltage up to 1000 V. There were two sets of HVE experiments with different types of electrolytic cells. The first set of experiments involved an electrolytic cell designed as a heat capacity calorimeter. The cell used in the second set of experiments was designed as a water-cooled flow calorimeter.

#### 1.1.1. Experiments with HVE Device as a Heat Capacity Calorimeter

The HVE device consisted of a quartz tube with an additional circuit for a working fluid. The anode and cathode units were placed inside the tube. To circulate the working fluid a mixer was installed inside the circuit. The quartz tube was also provided with a thermocouple.

The measurements of EH power were made proceeding from the assumption that no Excess Heat power is produced when using light water ( $H_2O$ ) with a Pd cathode system.

Considerable increase in EH power and Heat Efficiency was recorded for a Pd cathode pre-treated by saturation in  $D_2$ . EH power and Heat Efficiency values were lower in experiments involving a cell-calorimeter without thermal insulation (from the environment) (Fig.2a,b).

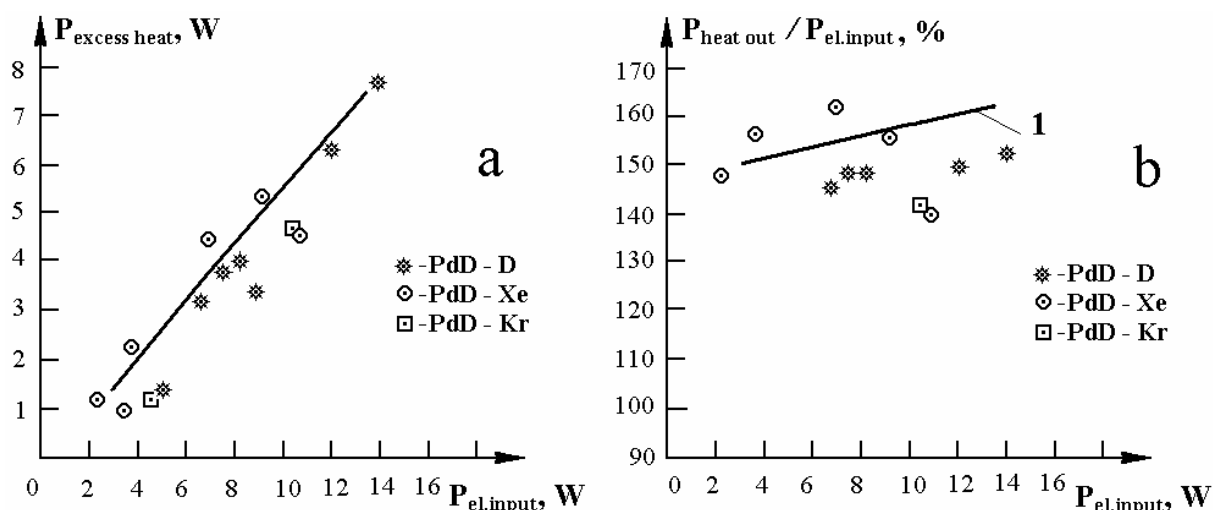


Fig.1. a - Excess Heat Power in relation to the input electric power. B - Dependence of the output heat power versus the input electric power ratio upon the input electric power. Pd cathode sample in  $D_2$ , Xe and Kr discharges.

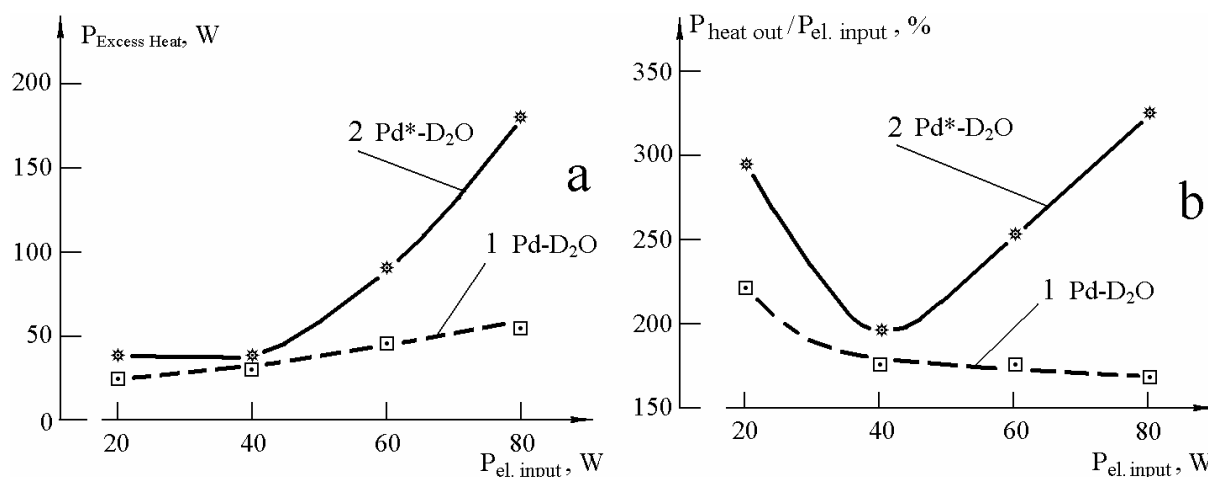


Fig.2. a - Excess Heat power value as a function of the input electric power. b - Dependence of Heat Efficiency value (correlation between the heat power output into the cathode water cooling system and the electric power input into the electrolytic cell) upon the input electric power: 1 – represents electrolysis in heavy water (D<sub>2</sub>O) with a Pd cathode (not pre-treated Pd); 2 – shows electrolysis in heavy water (D<sub>2</sub>O) with a Pd cathode (pre-treated Pd).

### 1.1.2.Experiments with HVE Device as a Flow Calorimeter

The HVE device (as a water-cooled flow calorimeter), consisted of a quartz tube with an additional circuit for a working fluid (Fig.18). The anode and cathode units were placed inside the tube. To circulate the working fluid a mixer was installed inside the circuit. One side of the flat cathode was washed by the working liquid, while the other side of it was cooled by the water flowing in a cooling tube. Thermocouples connected differentially were placed inside the water-cooling passage to take the difference in the cooling water temperature input and output.

Three sets of experiments were carried out at the following HVE operating parameters:

- 1) Electrolysis in light water (H<sub>2</sub>O) with a Pd cathode.
- 2) Electrolysis in heavy water (D<sub>2</sub>O) with a Pd cathode.
- 3) Electrolysis in heavy water (D<sub>2</sub>O) with a Pd cathode (pre-treated Pd cathode by saturation in heavy water for a month).

The Excess Heat power value in HVE based on light water (H<sub>2</sub>O) with a Pd cathode was assumed as zero.

Thus adapted experimental data is represented in Fig.3 (a,b).

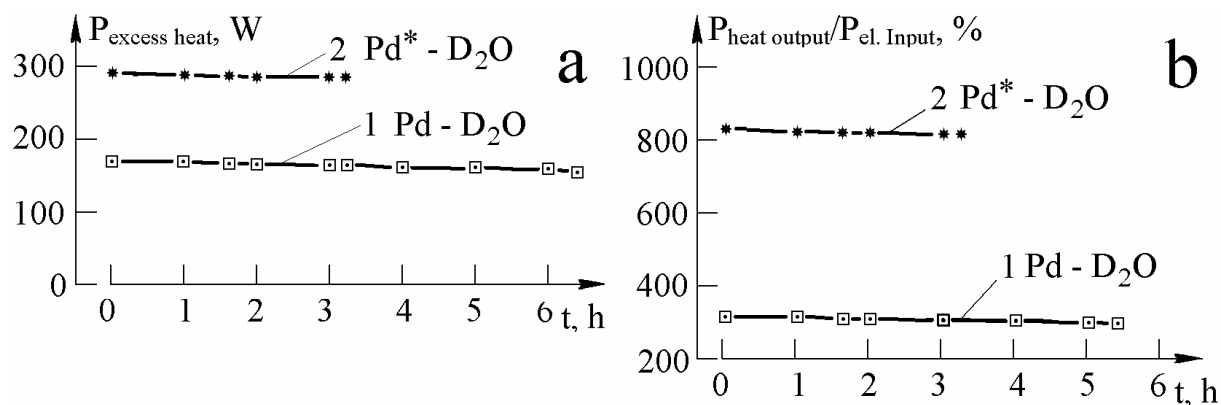


Fig.3.a- Excess Heat power value as a function of experimental time. b- Dependence of Heat Efficiency value (correlation between the heat power output into the cathode water cooling system and the electric power input into electrolytic cell) upon the experimental time 1 – represents electrolysis in heavy water (D<sub>2</sub>O) with a Pd cathode (not pre-treated Pd); 2 – shows electrolysis in heavy water (D<sub>2</sub>O) with a Pd cathode (pre-treated Pd).

## 2. IMPURITY NUCLIDES REGISTRATION

### 2.1. <sup>4</sup>He Impurity Registration

Presumably, the release of EH power is accounted for by <sup>4</sup>He production and the on-going reactions of transmutation accompanied by the impurity nuclides yield. <sup>4</sup>He had been registered in earlier experiments [1]. Some of Pd cathodes together with the reference samples were analyzed at the Rockwell International Laboratory (Oliver's group). A small increase in <sup>3</sup>He content and a large increase in <sup>4</sup>He concentration was found in Pd samples exposed to the discharge. The results of two experiments are represented in Table 1. This is the third independent evidence of <sup>4</sup>He presence in the nuclear reaction.

Table 1

The relative content of <sup>3</sup>He and <sup>4</sup>He in the cathode sample after exposure to GD. The cathode – plasma forming system is Pd – D<sub>2</sub>, the current value is 35 mA, the time of the exposure is 4 hours.

| # | <sup>3</sup> He <sub>after discharge</sub> / <sup>3</sup> He <sub>initial</sub> | <sup>4</sup> He <sub>after discharge</sub> / <sup>4</sup> He <sub>initial</sub> |
|---|---|---|
| 1 | up to 10 times  | up to 100 times   |
| 2 | up to 2 times   | up to 35 times  |

### 2.2. Impurity Elements Registration

The impurity elements content in the cathode samples was analyzed before and after the experiments with high-current GD Device.

The following methods were used: X-ray fluorescent spectrometry, spark mass spectrometry, secondary ionic mass spectrometry, and secondary neutral mass spectrometry. The impurity nuclides with a mass less than that of Pd and the impurity nuclides with a mass more than that of Pd were registered in the experiments.

The main recovered impurity nuclides (with more than 1% content) are  $^7\text{Li}$ ,  $^{12}\text{C}$ ,  $^{15}\text{N}$ ,  $^{20}\text{Ne}$ ,  $^{29}\text{Si}$ ,  $^{44}\text{Ca}$ ,  $^{48}\text{Ca}$ ,  $^{56}\text{Fe}$ ,  $^{57}\text{Fe}$ ,  $^{59}\text{Co}$ ,  $^{64}\text{Zn}$ ,  $^{66}\text{Zn}$ ,  $^{75}\text{As}$ ,  $^{107}\text{Ag}$ ,  $^{109}\text{Ag}$ ,  $^{110}\text{Cd}$ ,  $^{111}\text{Cd}$ ,  $^{112}\text{Cd}$ ,  $^{114}\text{Cd}$  (Fig.1). The total content of these impurities amounts to 1017, the experiment duration being up to  $2 \times 10^4$  sec. The observed change of natural isotope ratio for these impurity nuclides is up to several tens of times, some main isotopes of impurity elements (with high natural abundance percentage) being absent. The following isotopes were registered as being absent:  $^{58}\text{Ni}$ ,  $^{70}\text{Ge}$ ,  $^{73}\text{Ge}$ ,  $^{74}\text{Ge}$ ,  $^{113}\text{Cd}$ ,  $^{116}\text{Cd}$ .

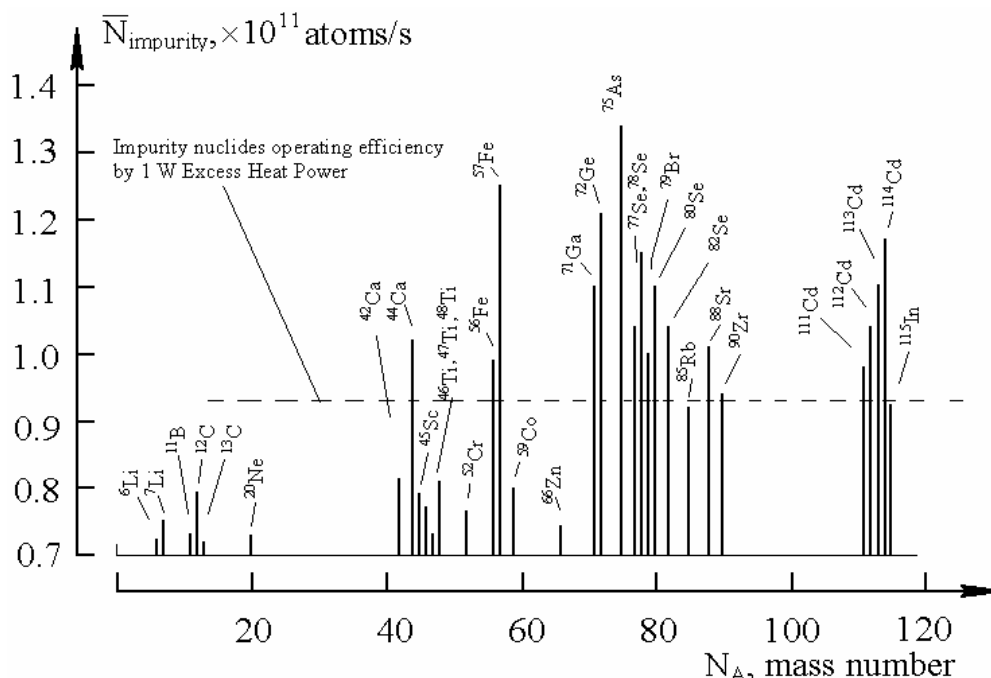


Fig.4. Intensity of operating time for impurity nuclides in the surface layer of 10  $\mu\text{m}$ -thick cathode sample. Pd – D2 experimental system, current –100mA, duration of experiment – 22 hours.

### 3. PENETRATING RADIATION ENERGY AND TEMPORAL CHARACTERISTICS

#### 3.1. X-ray Energy Registration

Two emission modes were revealed in the experiments: 1 - Diffusion X-rays were observed as separate X-ray bursts (up to  $10^5$  bursts and up to  $10^6$  X-ray quanta in a burst); 2 - X-rays in the form of laser micro beams (up to  $10^4$  beams per second and up to  $10^{10}$  X-ray quanta in a beam, with angular divergence being up to  $10^{-4}$ ). The registration of X-ray emission energy was performed using  $\text{Al}_2\text{O}_3$ -based TLD with absorbing Be foils of various thickness, PM scintillating

detectors (with absorbing Be foils). The X-ray spectra were recorded with the help of curved mica crystal X-ray spectrometer positioned on an X-ray film. The experimentally determined value of the X-ray energy increased from 1.5 to 2.0 keV when the thickness of Be shield increased from 15  $\mu\text{m}$  to 30.0  $\mu\text{m}$ . The X-ray energy values obtained by PM scintillating detectors (provided with 15  $\mu\text{m}$  and 30  $\mu\text{m}$ - thick beryllium foils) amounted to  $E_{\text{X-ray}} \approx 1.0 - 2.0$  keV. The spectrum was registered both as bands of the continuum with energies ranging 0.6 - 10.0 keV and as spots resulting from the emission of series of high-density mono-energetic X-ray beams (with energies up to 0.6 - 10.0 keV) characterized by small angular divergence. The said results showed good agreement with the TLD and PM scintillating detectors data (Table 1).

The spectrum band (ranging in energy 1.3 – 1.6 keV) was defined for Pd cathode samples in D<sub>2</sub> and Kr Glow Discharge (during its operation, and after, the discharge current switch off). This result is in good agreement with the maximum value of EH power at 1000 - 1300 V Glow Discharge voltage (Fig.5.).

Table 1.

| Method of X-ray emission energy measurement                         | Thermo-Luminescent Detectors with Be foils screen | Photomultiplier scintillating detectors with Be foils screen | Curved mica X-ray spectrometer                    |
|---|---|--|---|
| X-ray energy during the Glow Discharge Operation in Pd – D          | 1.3 – 1.8 keV                                     | 2.0 keV  | 1.7 – 1.8 keV<br>1.3 – 1.6 keV<br>0.81 – 0.84 keV |
| X-ray energy for Pd – D after the Glow Discharge current switch off |   | 1.7 keV  | 1.7 – 1.9 keV<br>1.4 – 1.6 keV<br>1.1 – 1.3 keV   |

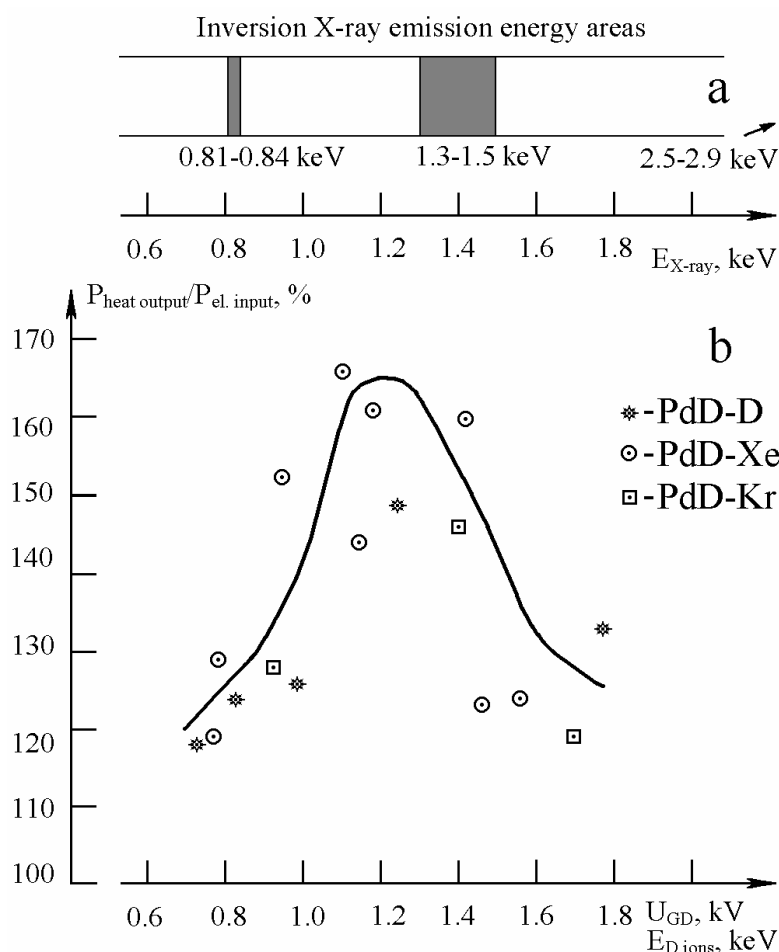


Fig.5. **a** - X-ray emission energy obtained by the curved mica crystal X-ray spectrometer. **B** - Dependence of the output heat power versus the input electric power ratio upon the Glow Discharge voltage (deuterium ions energy) . Deuterium pre-charged Pd cathode samples in  $D_2$ , Xe and Kr discharges.

### 3.2. X-ray Emission Temporal Characteristics.

X-ray emission as a function of time was studied with PM scintillating detectors.

The generation of X-rays began some time after the GD switch on. The delay in production of X-ray emission decreased with the increase in GD current and voltage (Fig.6.). The delay in production of X-ray emission was very small with high voltage Glow Discharge. Presumably, it takes some time for the solid medium to be activated and the inverse population to be created in the solid after the GD switch on.

The X-ray emission production occurred during the Glow Discharge operation, and, after the Glow Discharge current switch off . The X-ray beams were registered for some time after passing the GD current pulse trailing edge (Fig.7.). The time delay values were registered in the experiments. The temporal characteristic of the X-ray beams emission was determined for the following

conditions: zero point time corresponds to the GD current pulse trailing edge time, the number of X-ray beams was counted for each value of the time delay. The temporal characteristics of the X-ray beams emission shows the time delay as **fixed** values with  $\pm 2 \mu\text{s}$  deviation (Fig.8).

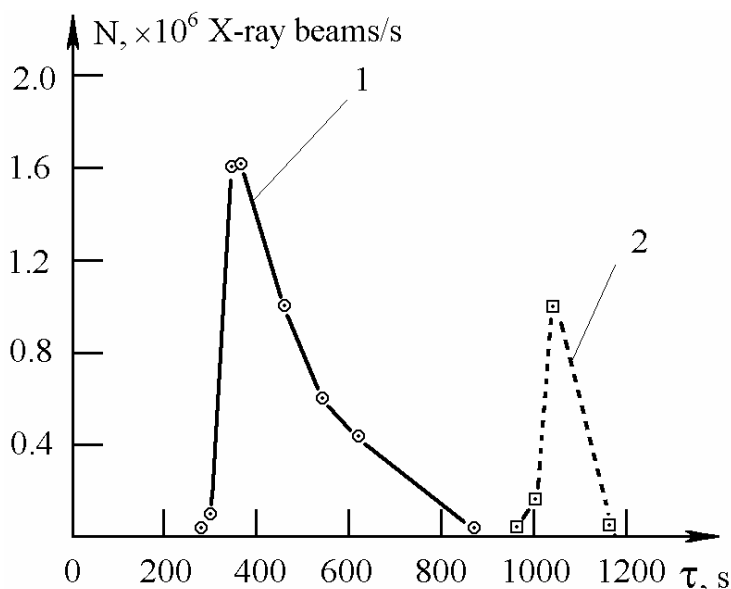


Fig.6. The time delay of X-ray beams emission for different Glow Discharge current and voltage parameters. 1 - current is 40 mA, voltage is 580 V, 2- 25 mA, 470 V.

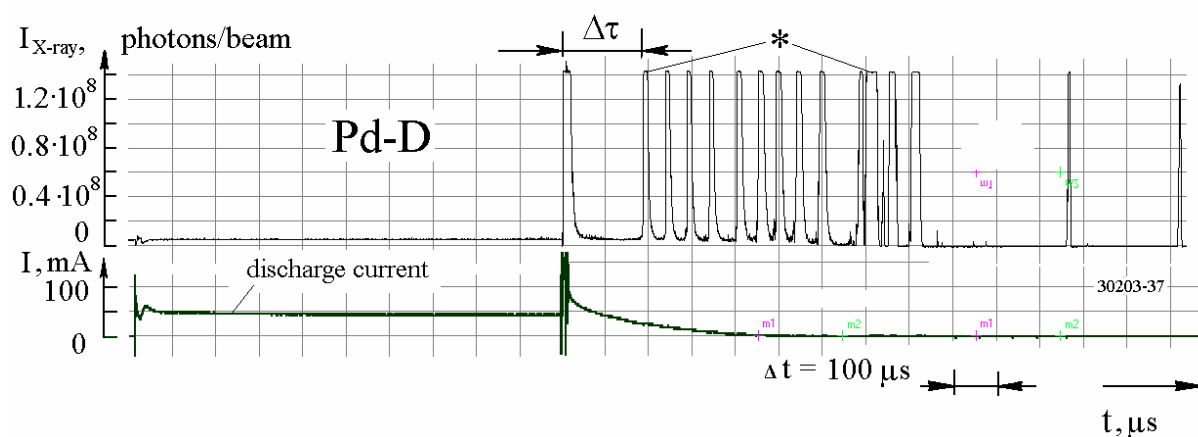


Fig.7. The typical oscillograms of bursts from X-ray laser beams (PM – scintillating detector). The cathode sample is Pd, D2 discharge, current - 50mA.



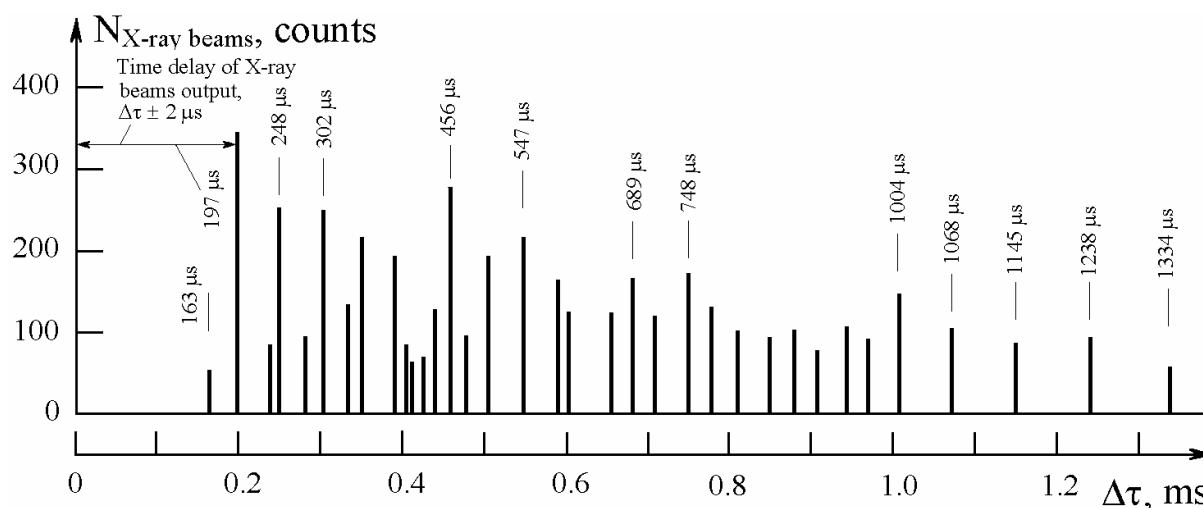


Fig.8. Temporal characteristic of the X-ray beam emission. The cathode sample is Pd, D2 discharge, current - 50mA.

#### 4. LOW ENERGY NUCLEAR REACTION PHENOMENON THEORY

The totality of experimental results permits one to consider a theoretical aspect of Low Energy Nuclear Reactions proceeding in the cathode solid medium exposed to the electric discharge systems.

The main experimental results are the following: The lifetime of long-lived excited states (with 1 -3 keV energy) is quite possible.

One can single out the following electric discharge areas and the physical phenomena observed within them:

##### I. Near cathode area of plasma or electrolyte.

Ions flux generation in electric discharge systems cathode area plasma or electrolyte. The transfer of electric discharge energy (1000-2000 eV) to ions flux of deuterium plasma. Bombardment of cathode solid surface by the ions flux.

##### II. Processes on the plasma-solid boundary and processes in the solid's superficial layer.

The soft collision  $D^+$  ions flux with surface of Pd cathode solid.

The following processes are observed:

- Anharmonic processes of "minor" low energy modes conversion to "mean" low energy modes (**P. Hagelstein process**).
- "Mean" low energy modes transfer in solid volume
- Creation of excited long-lived states with 1000-3000 eV energy in the solid medium;
- Deuterium loading into Pd solid.

##### III. Triggering and realization of Low Energy Nuclear Reactions in the solid.

##### IV. Conversion of nuclear reaction energy into the crystal lattice heat.

## I. Ions flux generation in plasma or electrolyte in the near cathode area of the electric discharge systems

In certain electric discharge conditions the positive discharge column is absent. Ion conducted layer is realized near the surface of Pd cathode solid, and almost all the cathode voltage drop value is used for ions acceleration. The electric discharge energy (1000-2000 eV) is transferred to ions flux of deuterium plasma.

## II. Processes on the plasma-solid boundary and processes in the solid's superficial layer.

Among processes of interaction between the ions flux and the solid's surface the process of solids' dispersion by ions bombardment (atoms knocking out of the crystal lattice by the ions flux) is now better understood.

Within the ions energy range of 2 keV each of the falling ions is capable of knocking out up to 2 atoms. The average crystal lattice atomic bond energy is about 10 eV. Thus the processes responsible for 1980 eV or 99% of the ions flux energy have not been adequately explored. Assumedly it is this energy which through interaction with electrons is converted into heat. The given LENR processes model is based upon a detailed scrutiny of interaction mechanisms between the falling ions flux and the crystal lattice. The basic assumptions and initial conditions are as follows.

The Pd crystal lattice is a face-centered cube with the lattice parameter being  $a = 0.389$  nm. The 4-valent Pd ions are characterized by the radius of  $r_{Pd^{4+}} = 0.064$  nm, the metal radius is  $r_{met} = 0.137$  nm. In the course of Pd saturation with deuterium the latter ions take their position among the Pd ions. The space between Pd and D ions is taken by free valence electrons. The cathode sample represents a mono crystal or a multi-mono crystal, i.e. it consists of separate grains, each being a mono crystal.

To assess the possible processes and their mechanisms one should evaluate spatial and temporal scale of phenomena observed. This will allow to define what particular occurrences should be taken into account. In the course of the crystal lattice bombardment by the ions of deuterium within the range of 1.0 - 2.0 keV the said ions velocity ( $v_{D+}$ ) for energy of 1 keV is equal to  $v_{D+} = 3.3 \cdot 10^5$  m/s.

Here  $v_{D+} = (2 \cdot W_{D+} / m_{D+})^{0.5}$ ;

$W_{D+}$  denotes the deuterons energy;  $W_{D+} = 1.103 \cdot 1.6 \cdot 10^{-19}$  J;  $m_{D+}$  is the deuteron's mass;  $m_{D+} = 3.34 \cdot 10^{-27}$  kg.

The time needed for deuterium ions to cover the distance equal to the lattice spacing is  $\tau_{D+} = a / v_{D+} = 1.2 \cdot 10^{-15}$  s. The relaxation time for electrons in metals (the electron free running time between collisions) is equal to  $\tau_R = (0.3-2) \cdot 10^{-14}$  s [8]. So, one can apply the solid plasma model. Deuterium ions interact with Pd ions through Coulomb's forces. Free valence conductivity electrons do not

have enough time to resume the state of equilibrium while D ion covers the elementary crystal cell spacing. At their approaching each other the minimum distance between a deuteron and a Pd ion defined by the Coulomb's repulsion can be determined by equalizing the D ion kinetic energy to the formed dipole potential energy.

$$\Delta_{rD+} = q_{D+} \cdot q_{Pd4+} / (4\pi\epsilon_0 W_{D+}).$$

For 1 keV energy  $\Delta_{rD+}$  is equal to  $5.8 \cdot 10^{-12}$  m. Here  $q_{D+}$ ,  $q_{Pd4+}$  represent D and Pd ions charges, correspondingly,  $\epsilon_0$  is an electric constant,  $W_{D+}$  – the deuteron's energy. The energy conveyed to Pd ion (in accordance with the elastic (recoil) collision model) is equal to:

$$W_{Pd4+} = W_{D+} \cdot 4 M_{D+} \cdot M_{Pd4+} / (M_{D+} + M_{Pd4+})^2 = 0.073 \cdot W_{D+}$$

The distance  $\Delta_{rD+} = 5.8 \cdot 10^{-12}$  m is very small as compared to the ion dimensions. Here interaction results in two possible occurrences: shift of Pd ion core from equilibrium lattice position, distortion and displacement of electrons shells relative to Pd nucleus. On approaching each other the ions repel and start moving in the opposite directions. This results in the oscillatory shift of Pd ion core from its normal equilibrium position within the lattice and oscillatory displacement of Pd ion electrons shells in relation to Pd nucleus. That is, the electric charge displacement by a  $\Delta r$  distance leads to formation of the electric dipole momentum  $p$ .

$$p = -e_0 \cdot r = 4\pi \cdot e_0 \cdot a^3 \cdot E_a$$

Here  $a$  stands for atomic radius,  $E_a$  represents the electric field caused by the lattice ions displacement in relation to valence electrons,  $\Delta r$  is the displacement value.

The oscillations associated with such local spatial charge division and the electric dipole momentum formation are viewed as optic polar phonons. Some oscillations may trigger macroscopic spatial division of charges and macroscopic polarization  $\mathbf{P}$  within the solid's volume.

$$\mathbf{P} = n_a \cdot \mathbf{p}. \text{ Here } n_a \text{ is the dipoles density.}$$

Macroscopic polarization in a solid leads to creation of macroscopic  $\mathbf{E}_a$  electric (current) field:

$$\mathbf{E}_a = (\mathbf{D} - \mathbf{P}) / \epsilon_0.$$

$\mathbf{D}$  - stands for electric induction.

The arising spatial division of charges causes a flow of valence electrons, which due to their small mass are characterized by high mobility and tend to neutralize the originated volumetric division of charges. These local flux of electrons are also of oscillatory character and are termed as plasmons. At oscillation frequencies being less than  $\omega_p$  ( $\omega_p$  is a plasma resonance frequency), free electrons have enough time to displace and compensate for the arising spatial division of charges. That is when generated with frequencies less than the plasma resonance frequency the optic polar phonons disappear, their energy being given away to free electrons. The electric field cannot penetrate deep

inside the metal. With regard to the process of the solid bombardment by the ions flow this implies deceleration of electrons and conversion of their energy into heat. The frequency of optic polar phonons being generated in experimental conditions can be estimated using the harmonic oscillator energy equation:

$$\omega_{op} = 2\pi \cdot \nu. \quad \nu = W_{op} / 2\pi \cdot h.$$

$h$  stands for the Plank Constant.

For the deutons' energy  $W = 1$  keV the frequency of a formed optic polar phonon is equal to

$\omega_{op} = 0.95 \cdot 10^{19} \text{ s}^{-1}$ . For a phonon formed by a Pd ion with energy of 0.077 keV  $\omega = 0.7 \cdot 10^{18} \text{ s}^{-1}$ . The plasma frequency  $\omega_p$  for metals [9]  $\omega_p = (2.1 - 3) \cdot 10^{15} \text{ s}^{-1}$ . Thus, it is quite possible that in the course of the cathode sample bombardment (in the said experimental conditions) the optic polar phonons with energies of (1.0 – 2.0) keV are generated, live for some short time and penetrate into the solid's body.

Plasma frequency  $\omega_p$  is defined by the following equation

$$\omega_p = (4\pi \cdot n_e \cdot e \cdot 2/m_e)^{1/2}$$

or by a more convenient digital expression [8]

$$\omega_p = (47.1 \text{ eV}) \cdot (r_s/a_0)^{-3/2}$$

Here  $n_e$  stands for conductivity electrons density,  $e$  is the electron charge,  $m_e$  represents electron mass,  $r_s$  denotes sphere volume radius per electron,  $h = 6.58 \cdot 10^{-15} \text{ eV} \cdot \text{s}$  is the Plank Constant.

For metals [9]  $\omega_p = (1.3 - 2.5) \cdot 10^{16} \text{ s}^{-1}$ . The frequency of primary optic polar phonons arising from solid bombardment by ions with energies of (1.0 – 2.0) keV is defined as  $\omega_{op} = 1.0 \cdot 10^{19} - 1.5 \cdot 10^{19} \text{ s}^{-1}$ , the former being much bigger in value than the plasma frequency  $\omega_p$ . These estimations show that the conditions for existence of primary optic polar phonons generated in ion bombardment are met and they last for a certain lifetime. The oscillation amplitude for such optic phonons is determined by the formula:

$$\Delta x = (2 \cdot W_{op} / m_i (\omega_{op})^2)^{1/2}$$

Here  $m_i$  stands for the ion mass.

For a Pd nucleus oscillating relative to its electron shell at energy of 1.0 keV the amplitude  $\Delta x_{Pd}$  is equal to:  $\Delta x_{Pd} = 1.0 \cdot 10^{-13} \text{ m}$  (the nucleus size  $\approx (3-5) \cdot 10^{-12} \text{ m}$ ).

The local electric field intensity  $E_{loc}$  resulting from the displacement of both the electron shell and the nucleus is characterized by a very big value because the distance between the electric charges is very small. At the said electric field frequency being higher than plasma frequency the electric induction value is close to zero. The electric field intensity is identified by the number of dipoles being formed. The macroscopic electric field intensity  $E_a$  builds up with the increase in the number of atoms  $n_a$  assuming the state of polar phonon excitation (the dipoles number):

$$\mathbf{E_a} \sim n_a \cdot \mathbf{E_{loc}}$$

At big values of macroscopic electric field intensity  $\mathbf{E_a}$  the largest share in the distribution of energy is taken by non-linear (enharmonic) occurrences. The medium dynamic polarization can be represented as follows:

$$\mathbf{P} = \epsilon_0 \cdot (\chi_1 \mathbf{E_1} + \chi_2 \mathbf{E_1}^2 + \chi_3 \mathbf{E_1}^3 + \dots)$$

Here  $\mathbf{P}$  denotes environment polarization,  $\chi_1, \chi_2, \chi_3..$  stand for non-linear media susceptibilities. The intensity of non-linear processes is determined by the following members:  $\chi_2 \mathbf{E_1}^2, \chi_3 \mathbf{E_1}^3, \dots$ . In the general case  $\chi_2, \chi_3$  susceptibilities are defined by the kind of material, type and state (physical parameters) of the crystal lattice.

Assumedly, the processes of the third (13) and the fourth (14) order play an essential part here:

$$h^* \omega_{1pr} + h^* \omega_{2pr} \rightarrow h^* \omega_3 \quad \text{And} \quad \omega_1 < \omega_3 > \omega_2$$

$$h^* \omega_{1pr} + h^* \omega_{2pr} + h^* \omega_{3pr} \rightarrow h^* \omega_4 \quad \text{And} \quad \omega_1 < \omega_4 > \omega_2, \quad \omega_4 > \omega_3$$

Here  $h^* = h/2\pi$

Expressions mean that two  $h^* \omega_{1pr}, h^* \omega_{2in}$  or three primary phonons  $h^* \omega_{1pr}, h^* \omega_{2in}$  and  $h^* \omega_{3pr}$  merge and form a new one  $h\omega_3$  or  $h\omega_4$ . The frequency of the newly formed phonons and consequently their energy  $\mathbf{W_{op}} = h \cdot \omega_{op} / (4\pi^2)$  will be bigger in value. In this way out of a big number of primary phonons with energies of (1.0 – 1.5) keV a smaller amount of high-energy phonons (up to tens and hundreds keV) is formed. The energy spectrum of primary phonons is shifted to high energies. Presumably, one of the most essential occurrences within the energy range of more than 1.0 keV is the energy transfer from optic polar phonons to electrons of the crystal lattice L-, M- and K- electronic atomic shells. There is experimental data proving the existence of such mechanism for energy conversion: registration of high current and voltage pulses of millimicrosecond length. The energy spectrum of these high-voltage pulses is linear in character and is shifted in the direction of high energies proportional to the current density increase. The pulses result from outburst of beams of fast electrons with L-, M- and K- shells, that have acquired their energy from high-energy optic polar phonons. This process should be accompanied by emission of specific X-ray radiation or Auger - electrons emission due to electron transfer from the higher shell to a vacant place in the lower electron shell. Rather intensive X-ray radiation is registered in the course of experimentation.

It should be noted that Pd crystal lattice is “cold” (300–400) °K, Pd ions are placed at the lattice points and perform heat oscillations, corresponding to the said temperature. D ions are also spatially fixed among Pd ions though the energy of this bond is not so big (~0.05eV). But Pd ions are in a state of optic polar oscillatory excitation with energies up to tens and hundreds keV. An environment characterized by unbalanced excitation of one of its energetic states

is created. In laser physics it is common practice to define a particular energetic state by its specific temperature. In this case one can assume that the Pd crystal lattice is characterized by a heat oscillation (fluctuation) temperature of  $T_{\text{crys}} = (300-400)^\circ\text{K}$  and by the optic polar phonon temperature of  $T_{\text{opph}} > 3.0 \text{ keV}$  ( $> 30\,000\,000^\circ\text{K}$ ,  $1\text{eV} = 11000^\circ\text{K}$ ).

### **III. Triggering and realization of Low Energy Nuclear Reactions in the solid.**

These data refer to balanced nuclei excitation but there is experimental evidence proving that the cross-section of nuclear reactions for nuclei with unbalanced excitation is expanding.

The assumed model of the involved processes is the following:  
 The Pd crystal lattice is “cold” (on account of the cathode sample cooling).  
 The Pd ions are fixed in the crystal lattice points and perform heat oscillations, corresponding to the cooling temperatures. But Pd ions are also subject to optic polar fluctuations relative to their electrons shells with energies up to 10 keV (the mechanism for triggering the latter fluctuations is described above).



The non-equilibrium excited energy states with the population density of  $n_{\text{exit}}$  [ $\text{cm}^{-3}$ ] and a characteristic temperature of  $T_{\text{exit}} \approx 1.0 - 3.0 \text{ keV}$ , and more, were formed the conditions for the Low Energy Nuclear Reaction realization.

To determine the specific physical mechanism for these reactions requires some additional research. One possible type of reaction for forming the impurity nuclides can be long-range (resonant) nuclear reactions [3].

The following types of nuclear reactions of transmutation resulting in formation of stable nuclides are possible:

- 1)  $\text{Pd} + m\text{D} \rightarrow [\text{PdmD}]^*$
- 2)  $[\text{PdmD}]^* \rightarrow \text{D}^* + {}^4\text{He} + \text{Heat}$
- 3)  $[\text{PdmD}]^* \rightarrow \text{A}^* + \text{B}^* \rightarrow \text{A} + \text{B} + \text{Heat}$
- 4)  $[\text{PdmD}]^* \rightarrow \text{C} + \text{Heat}$

Where  $[\text{PdmD}]^*$  is a short-lived intermediate compound nucleus;  $m=1,2,3 \dots$ ;  $\text{A}^*, \text{B}^*$  denote nuclear isomers of nuclides with masses less than that of Pd;  $\text{A}, \text{B}$  are stable nuclides;  $\text{C}$  stands for a nuclide with a mass more than that of Pd. At first a composite compound-nucleus in excited state is formed. Then one of the three possible modes is realized:

1) the compound nucleus may lose its excitation and form an excited Pd nucleus and  ${}^4\text{He}$ .

2) the compound nucleus may split into two nuclei fragments with masses less than that of Pd. In so doing the two nuclei should be in excited isomer state (experiments show that the nuclear reactions energy is not produced in the form of nuclear fragments kinetic energy).

3) the compound nucleus may lose its excitation and form a stable nucleus of a heavier than Pd element.

#### **IV. Conversion of nuclear reaction energy into the crystal lattice heat.**

The last stage of the process involves conversion of nuclear reaction energy into heat. Assumedly, relaxation of the compound-nucleus or isomers' excited state proceeds on account of multi-stage transitions involving energy transfer to all the macro-monocrystal atoms (up to  $10^8$ ) at each transition stage by means of multi-phonon processes.

Acoustic phonons (recoiling sound wave) interacts with all the macro-monocrystal atoms during one nuclear transition stage converting this energy into energy of crystal lattice heat oscillations.

All these stages are presented in the diagram (Fig.9).



## 5. CONCLUSIONS

The development of new nuclear engineering is possible based on low energy nuclear reactions in the solid-state medium. This type of engineering can be called "Third way" in nuclear engineering in comparison with the nuclear engineering based on uranium nuclear fission, and thermonuclear synthesis.

## REFERENCES

1. A.B. Karabut, Ya.R. Kuchеров, I.B. Savvatimova, "Nuclear Product Ratio for Glow Discharge in Deuterium", *Physics Letters A*, 170, p.265,1992.
- 2.A.Karabut, "Heat Energy Production Method", Patent #2240612, 20 November, 2004, Russian Federation.
3. A.B.Karabut, "RESEARCH INTO LOW ENERGY NUCLEAR REACTIONS IN CATHODE SAMPLE SOLID WITH PRODUCTION OF EXCESS HEAT, STABLE AND RADIOACTIVE IMPURITY NUCLIDES", Proceedings of the 12<sup>th</sup> International Conference on Cold Fusion, December 2 – 7, 2006, JAPAN.
4. A.B.Karabut, "STUDY OF ENERGETIC AND TEMPORAL CHARACTERISTICS OF X-RAY EMISSION FROM SOLID-STATE CATHODE MEDIUM OF HIGH-CURRENT GLOW DISCHARGE", Proceedings of the 12<sup>th</sup> International Conference on Cold Fusion, December 2 – 7, 2006, JAPAN.
5. G. Kazyonov at all, "Experiments of anomalous output heat registration by electrolysis in heavy water", PROCEEDINGS of the 10-th RUSSIAN CONFERENCE ON COLD NUCLEAR TRANSMUTATION OF CHEMICAL ELEMENTS AND BALL LIGHTNING, DAGOMYS, CITY OF SOCHI, September 29 – October 6, 2002, Russia, pp. 41 – 49.
6. A.V.Yeremeyev, at all "Experiments of anomalous output heat registration by high voltage electrolysis in heavy water (method detail)", PROCEEDINGS of the 12-th RUSSIAN CONFERENCE on COLD NUCLEAR TRANSMUTATION of CHEMICAL ELEMENTS and BALL LIGHTNING, DAGOMYS, CITY OF SOCHI, September 19 –26, 2004, Russia, pp. 98 – 108.
7. P.Grosse, "Free Electrons in Solid", Springer-Verlag, Berlin-Heidelberg-New York, 1979, p.191-217.
8. Neil W. Ashcroft, N.David Mermin, "Solid State Physics", Cornell University, Holt, Rinehart and Winston, New York, 1976, v.2, p.116-137.